JGR Earth Surface

RESEARCH ARTICLE
10.1029/2020JF005773

Morphology, Bedload, and Sorting Process Variability in Response to Lateral Confinement: Results From Physical Models of Gravel-bed Rivers

Costanza Carbonari[1,2], **Alain Recking**[2], and **Luca Solari**[1]

[1]Dipartimento di Ingegneria Civile e Ambientale, Università Degli Studi di Firenze, Firenze, Italy, [2]INRAE, UR ETNA, Université Grenoble Alpes, Grenoble, France

Key Points:

- We perform flume experiments to represent poorly-sorted gravel-bed rivers with the same active channel width but different extents of lateral confinement
- Channel morphologies, geometries, sorting patterns, and bedload transport rates are strongly influenced by lateral width constraints
- Among the three configurations tested, the one with intermediate width confinement promotes a single-thread to braided pattern and presents less variation in sediment transport rate

Correspondence to:
C. Carbonari,
costanza.carbonari@unifi.it

Citation:
Carbonari, C., Recking, A., & Solari, L. (2020). Morphology, bedload, and sorting process variability in response to lateral confinement: Results from physical models of gravel-bed rivers. *Journal of Geophysical Research: Earth Surface*, *125*, e2020JF005773. https://doi.org/10.1029/2020JF005773

Received 3 JUL 2020
Accepted 9 OCT 2020
Accepted article online 17 OCT 2020

Abstract This paper uses flume experiments to investigate the influence of lateral width confinement on channel morphology, sediment sorting, and bedload transport. Three runs of about 60 hr were carried out under constant feeding rate equal to 0.6 l/s and 8 g/s, with a bimodal mixture of natural sediments, a fixed flume slope of 3%, and width imposed by lateral walls from 0.12 to 0.50 m in order to model three different flow confinement configurations. Despite the three runs transporting at the same rate on average, they presented different gravel-bed river morphologies and different degrees of bed complexity. The three runs also presented differences in bedload transport rate fluctuations associated with different magnitude and mechanisms of bed storage and release of sediments. The intermediate width configuration (Run 2) was found to have a minimum storage and release of sediments compared with both the wider configuration (Run 1) and the narrower configuration (Run 3). Runs 1 and 3 were characterized by a significant storage and release of sediments resulting in a highly fluctuating bedload transport rate; however, while Run 1 (braiding morphology) stored and released sediments through lateral deposits and bed variations with planimetric sorting, Run 3 (single-thread channel) stored and released sediments through variations in bed elevation accompanied by vertical sorting. We extrapolated this concept to the full set of gravel-bed river morphologies, thus speculating about the channel morphology for optimal sediment transfer.

1. Introduction

Gravel-bed rivers are self-formed channels in coarse alluvial substrata; their dynamic results from the feedback between the flow and the morphology through sediment transport (Church, 2006, 2010). Sediment transport in gravel-bed rivers occurs in the form of suspended load and bedload, the latter being the transport mode which has a major role in shaping the channel morphology (Church, 2006); bedload transport is also characterized by an unsteady, intermittent nature (Gomez et al., 1989; Kuhnle, 1996; Singh et al., 2009). Indeed the pulsating character of bedload transport in gravel-bed rivers has been observed also under steady flow conditions (Dhont, 2017; Recking et al., 2009); furthermore, bedload transport varies depending on sediment supply (Madej et al., 2009; Recking, 2012; Yager et al., 2012). Moreover, it has been shown that bedload transport rate is strongly affected by the spatial variation of both shear stress (Ferguson, 2003; Francalanci et al., 2012) and critical shear stress (Ferguson, 2003; Nelson et al., 2009; Venditti et al., 2008).

The treatment of bedload transport in nonuniform channels is not an easy task because of lateral variability of flow condition and hence shear stress, and nontrivial issues can arise when adopting a 1-D model (Ferguson, 2003; Recking et al., 2016). Lateral variability in hydraulic condition across a river is due to different depth and flow structures inherited from upstream, and this is shown to affect bedload transport rate: in particular Ferguson (2003) argued that bedload flux increases greatly with the variance of the bed shear stress, especially in gravel-bed rivers. Actually, lateral variability of the flow field is relevant in gravel-bed rivers which are characterized by complex bed topography including riffle and pool sequences, bars, and braiding; it seems therefore compelling to study bedload transport in relation to channel morphology, and in so doing the dependence of bedload transport rate on lateral variability of shear stress is analyzed from a local scale (cross-section) to a wider morphological reach scale. Previous observations and theories on regime width for live-bed gravel channels are those of Bagnold (1977), Bagnold (1980), Carson and Griffiths (1987), Henderson (1966), and Parker (1978) in which the authors explored the relationship

between bedload transport and channel width. According to Bagnold (1977, 1980), and Parker (1978), for a given flow discharge, wider channels have greater gravel transport, whereas Henderson (1966) found the opposite to be true. Carson and Griffiths (1987) affirmed that an optimal width exists which maximizes bedload transport. Carson and Griffiths (1987) made a further step questioning whether a braided river, for given flow discharge, slope, and bed material, has a greater bedload transport than a single-thread river. In this regard, Francalanci et al. (2012) explored the effect of the alternate bar morphology on bedload transport rate by comparing 3-D computation of bedload transport over alternate bars against transport in a 1-D flat-bed uniform channel; 1-D and 3-D computations were conducted using the same slope and the same average flow velocity. In the two cases they inferred the sediment transport rate and the flow resistance; in particular, the comparison is enabled by the fact that for the numerical model with bars, the resulting sediment transport and the flow resistance are averaged over the bar wavelength. The authors introduced a correction consisting of the morphological factor k_q quantifying the overall deviation of average bedload transport when averaged over an alternate bar wavelength, as compared to the equivalent 1-D case: where is the "average over a bar pattern" of the local values of the bedload and q is the bedload given by a generic 1-D computation. The parameter k_q was investigated at varying discharge, water level, and flow velocity and the cases of $k_q > 1$ (bedload transport rate enhanced) were identified. Precisely, local sediment transport increases ($k_q > 1$) because of increased velocity occurring in deeper regions on the bar pattern, and k_q values become larger for decreasing values of the ratio between shear stress and critical shear stress. Francalanci et al. (2012) concluded that alternate bars can strongly enhance bedload transport at low Shields stress, which is a common condition in gravel-bed rivers. The same line of research was pursued by Recking et al. (2016) whose objective was to extend the notion of "morphologically averaged" bedload to different river morphologies (sand bed, riffle-pool, plane bed, and braiding). This was achieved through a comparison between a reference state consisting of bedload function derived in flat-bed narrow flume, and field measurements of bedload in different bed morphologies. Recking et al. (2016) concluded that bedload transport rate variability due to morphology is important for low transport stage, where the Shields stress is just above the threshold condition for transport. Moreover, for a given grain shear stress, greater lateral variability of bed topography results in a larger mismatch between the field measurements of bedload rate and the bedload rate computed through flume-derived equations. Both Francalanci et al. (2012) and Recking et al. (2016) considered the effect of morphology on bedload transport rate only in terms of bias between the transport rate characterizing a given morphology and the transport rate characterizing a flat-bed reference configuration. We lastly point out that both the studies did not investigate changes in critical shear stress due to grain size heterogeneity and sorting, which is in general scarcely investigated in wide gravel-bed river morphologies (namely the morphologies characterized by low lateral flow confinement) (Leduc, 2013).

Bedload transport rate also depends on changes in critical shear stress due to grain size heterogeneity and the resulting common formation of patterns of sorted sediments in the channel bed (Ferguson, 2003). This is a key aspect in gravel-bed rivers since they have a grain size distribution typically characterized by poorly sorted sediments (Cudden & Hoey, 2003; Iseya & Ikeda, 1987; Mosselman, 2012; Parker, 2008; Parker et al., 1982). These distinct size fractions of sediments interact differently with flow: During bedload transport, heterogeneous sediments typically undergo the process of sorting so that the grain size distribution of river beds displays significant spatial structures both in the surface texture (Nelson et al., 2009) and in the stratigraphy (Bacchi et al., 2014), giving rise to several kinds of patterns occurring at different spatial scales (river profile, reach, unit). These patterns typically develop both in the plane (e.g., surface patchiness in Nelson et al., 2009, 2015; Venditti et al., 2008) and in the vertical direction (e.g., armoring in Bacchi et al., 2014, among others). Bed surface and subsurface heterogeneity may also be a primary control on sediment transport rate (Ferguson, 2003; Iseya & Ikeda, 1987; Recking et al., 2009), and because bed material exerts a strong control on the near-bed hydraulic environment, patches may have important implications for aquatic ecology (Jähnig et al., 2009; Weber et al., 2009). Moreover, sediment segregation patterns in gravel-bed rivers can also have complex feedbacks with both slope and channel width adjustments, as is the case in flows with a low lateral confinement (Lisle et al., 2000).

A further issue is the effect of different width constraints on river bed topography and morphology (Garcia Lugo et al., 2015; Mueller & Pitlick, 2014) and sorting dynamics of poorly sorted sediments. Figure 1 illustrates field evidence of the influence of lateral confinement on river morphology; the photo captures the Séveraisse in the south of France, from an upstream braided reach the river width is abruptly and drastically

Figure 1. The Séveraisse River, south of France; 44°49′28″ N, 6°9′6″ E. The reach framed in the photo has a slope of about 1.5% and a daily discharge of 10–30 m^3/s. The upstream part of the reach has a braided morphology, channels adjustments occur in the plain, planimetric sorting is present (poorly sorted sediments D_{50} = 37 mm, D_{84} = 113 mm; patches of fines and coarse deposits). Downstream embankments force the river to a narrow single-thread morphology characterized by vertical channel adjustments, armoring (D_{50} = 110 mm, D_{84} = 303 mm), and no planimetric changes nor sorting.

reduced by embankments, forcing the river to a narrow single-thread morphology. Some studies have considered the effect of different widths on alternate and multiple bar formation (Fujita, 1989) or on braided river sediment transport (Marti & Bezzola, 2006), but detailed investigations on morphological changes due to lateral confinement are rare (Garcia Lugo et al., 2015; Mueller & Pitlick, 2014). There are very few studies that considered how lateral confinement affects both channel morphology and sorting. Among them, the field work by Mueller and Pitlick (2014) primarily aimed at testing a sediment supply braiding threshold on 53 gravel-bed channels, and secondarily provided observations on channels' pattern depending on channel lateral constraint. Precisely, the authors observed that, in conditions of sediment continuity and constant slope, longitudinal alternations of braided and single-thread reaches are governed by channel constriction; moreover bed sediment coarsens more in single-thread reaches than in braided ones. The experimental observations by Garcia Lugo et al. (2015) showed that small changes in channel width can have significant impacts on bed form and spatial variability. These results confirmed the well accepted theory of stability analysis for bar formation (Colombini et al., 1987): for a given discharge, reach slope, and bed material, the increment of the width-to-depth ratio has the effect of exciting increasing bar transversal modes (m = 1 alternate bars, m = 2 midchannel bars, m = 3 multiple bars) corresponding to a greater complexity of the river bed; this applies up to the theoretical limit of unconfined flows (width-to-depth ratio $\rightarrow\infty$) corresponding to braided systems. Garcia Lugo et al.'s (2015) results are relevant to the prediction of future river states, illustrating that any changes in river width impacts the form of the channel bed and the distribution and diversity of physical habitats that are present. However, Garcia Lugo et al. (2015) explored the effects of lateral constraint on channel morphologies performing experiments with uniform sediments; and hence, once again, the role of sorting processes was not taken into account in gravel-bed rivers' morphodynamics.

Garcia Lugo et al.'s (2015) results have direct relevance to river restoration, since they indicated that even small increases in channel width can have beneficial effects for bed complexity and thus morphological quality. Actually, river widening and channel reconfiguration are well-accepted and widespread restoration actions in response to a recent mandate to achieve good ecological status of water bodies: an increase in river lateral mobility is needed to improve bed morphological complexity and ecological quality (e.g., Rohde et al., 2004, 2005). In fact, river reaches with wider channels that promote the formation of local sediment deposits and gravel bars, or reaches with greater sediment inputs enhancing sediment heterogeneity, can foster river ecological habitat and biodiversity (Martín et al., 2018); whereas stable river reaches are characterized by low habitat turnover (Jähnig et al., 2009). Several field studies confirmed such restoration strategies and their effects (e.g., Jähnig et al., 2009, 2010; Martín et al., 2018). A clear example is the case of the Thur River in Switzerland studied by Martín et al. (2018) who investigated the effect of protection (lateral levees, etc.) removal on ecosystem structure and function 12 years after dechannelization. Embankments removal resulted in the formation of new gravel bars. The authors especially focused on biotic aspects by measuring hyporheic sediment respiration, macroinvertebrate density, and taxa richness, and they observed

that ecosystem structure and function presented complex responses in relation to flow-restoration feedback that are usually absent in channelized streams due to more stable conditions in sediment and flow regimes. The overall conclusion is that restoration enhanced ecosystem heterogeneity of hyporheic sediments in the Thur River.

The aim of the present work is to address some of the research gaps described above about the interaction of channel morphology, bedload, and sorting by investigating the effect of lateral confinement on morphodynamics of gravel-bed rivers and in particular on bedload transport and grain sorting processes. Three experiments in dynamic equilibrium conditions, having the same flow and sediment discharge, the same longitudinal slope, the same sediment mixture, but different lateral confinement, were performed to answer the following research questions:

- To what extent do bed morphology and channel geometry, the latter evaluated in terms of slope and active channel width, vary in response to different lateral width constraints? This question is posed in the attempt to provide quantitative information useful in river management, given that design strategies adopted in river restoration increasingly reflect the view that an increase in river lateral mobility is needed to improve bed morphological complexity and ecological quality, but still in this field a rather empirical approach is often adopted.
- To what extent do surface and vertical sorting patterns change in response to different channel width constraints? This question is posed because it provides a first step toward understanding the impact of change in flow lateral confinement on spatial scales and patterns of bed surface and subsurface sediments, the latter having a primary control on sediment transport rates.
- What is the effect of lateral confinement on bedload transport rate fluctuations? Are there any configurations and morphologies characterized by a sediment transfer that varies greatly in terms of magnitude and frequency? And, on the other hand, are there any river morphologies which in contrast are characterized by a more constant sediment transport? In this sense, among the gravel-bed river morphologies, does a channel configuration with an optimal sediment transfer exist?

This paper is organized as follows. Section 2 describes the experimental setup and methodology. Section 3 is devoted to results and analysis; in particular, sections 3.1 and 3.2 describe channel morphology and sorting patterns in the three experiments; section 3.3 provides for the three runs the acquired data illustrating oscillations of surface sediment composition, bed slope, and sediment transport rate despite steady external conditions; section 3.4 investigates the feedback between surface sediment composition, slope, and transport rate for each run; while section 3.5 goes back to the entire set of experiments analyzing the data provided in section 3.3 with a focus on their variability; lastly, section 4 provides an interpretation of such variability (section 4.1), and extends previous consideration to overall channel morphologies (section 4.2). Finally, section 5 draws conclusions.

2. Methods

The research activity of the present work was carried out through an experimental approach. Three runs of about 60 hr were carried out in a 6-m-long flume with a maximum width of 0.5 m, located at the Inrae (French National Institute for Agriculture, Food, and Environment) Grenoble Centre, France. The three runs modeled flow and morphological conditions typical of steep gravel-bed rivers and did not reproduce a particular field prototype. We chose a steep configuration because this responds to a management concern frequently encountered in narrow and densely populated alpine valleys, and also because it corresponds to a compromise allowing access to an observation of topographic changes which would have occurred over too long times at low slopes. The three runs were carried out under constant feeding rate conditions. The long duration of each experiment ensured a dynamic equilibrium between sediment transport within the channel, sediment exiting the flume, and channel bed morphology. This enabled us to follow the morphodynamic evolution of the bed for a representative time interval, and to achieve long time series of the collected data. Each entire run is considered in equilibrium conditions since before the duration of 60 hr we ran each experiment for several hours in order to let the bed adjust to its equilibrium slope in each specific flume width configuration. During such adjustment phase we measured the bed slope and the outlet sediment discharge; when the average value of the latter equalled the constant value of the inlet sediment discharge we began the actual experiment with its complete data acquisition. Our experimental equipment allowed for high-resolution measurements of the bed surface sediment composition, whereas the measurements of the

Table 1
Grain Size Characteristics of the Bimodal Mixture and of the Single Fractions[a]

	Fine fraction	Coarse fraction	Mixture
D_{16} (mm)	0.6	1.4	0.7
D_{50} (mm)	0.7	1.8	1.5
D_{84} (mm)	0.9	2.2	2.1
σ(_)	1.23	1.25	1.53

[a]Standard deviation evaluated as $\sigma = \frac{1}{2}\left(\frac{D_{84}}{D_{50}} + \frac{D_{50}}{D_{16}}\right)$.

bedload transport rate and the bed slope had a lower resolution, namely larger sampling time as illustrated in the following (section 2.2). High-resolution monitoring of the bedload transport rate and the bed topography is important when the research goal is multiple time scales of fluctuations of the bedload transport rate and the bed slope (Dhont, 2017; Dhont & Ancey, 2018; Kuhnle & Southard, 1988; Singh et al., 2009), and it has been shown that fluctuations and statistics of bedload transport rate present a sampling-time dependence (Fienberg et al., 2010). Investigations on the scale-dependent nature of transport rate is beyond the scope of this work; we nevertheless make use of time series of the bedload transport rate sampled with 20-min time intervals.

2.1. Experimental Setup

The flume had a fixed slope of 3.18% (this slope was inspired by the work of Lisle et al. (1991) that we used as a reference at the beginning of this study) and we set in the entire flume a layer of well mixed sediments which constituted the erodible mobile bed. This layer was composed of the same bimodal sediment mixture used for the inlet sediment discharge; 60% of the mixture consisted of a coarse fraction, characterized by a D_{50} equal to 1.8 mm; the remaining 40% was the fine fraction which had a D_{50} equal to 0.7 mm. Each fraction was rather homogeneous; the characteristic grains sizes and standard deviation of the two fractions and of the resulting mixture are reported in Table 1. Each experiment was conducted within a fixed-width channel: 0.5, 0.25, and 0.12 m for Runs 1–3, respectively (Table 2). The lower widths were achieved by placing between the fixed flume walls a third movable wall set at the required distance from one fixed wall. We stuck on the walls the fine gravel constituting the coarse fraction of the sediment mixture used, thus when the flow was against the walls it always experienced an appropriate roughness and no flow acceleration occurred (avoiding local exaggerated scouring). The three experiments were performed with the same steady water and sediment feed rates: 0.6 l/s and 8 g/s (Table 2). Experimental conditions ensured bedload transport of both the sediment fractions in the active channel. The sediment system had no recirculation in order to maintain a constant composition of the sediment mixture; at the upstream section the sediments enter the channel from a volumetric sediment feeder at a constant rate. Sediments were collected at the flume outlet, separated from water through a sieve placed in a bucket and, once roughly drained, weighed. The water content has been corrected by weighing dried samples.

In the wider flow configurations, Runs 1 and 2, there were also wetted areas which are areas with flowing water and no sediment transport, and dry areas, that were emerged zones. In fact, in Runs 1 and 2 the active channel could wander in the large alluvial bed because of the relaxation of the lateral constraint:

Table 2
Summary Data of the Experimental Runs[a]

Run #	T (hr)	Q (l/s)	Q_s (g/s)	W (m)	S (m/m)	Active width (m)	h (m)	U (m/s)	Fr	θ/θ_c
1	60	0.55	8	0.5	0.034 (→0.031)	0.12	0.01	0.46	1.19	1.65–4.02
2	60	0.57	8	0.25	0.032 (→0.026)	0.12	0.011	0.43	1.31	1.44–3.52
3	60	0.59	8	0.12	0.032 (→0.025)	0.12	0.012	0.41	1.46	1.5–3.68

[a]T, run duration; Q, inlet water discharge; Q_s inlet sediment discharge; W, flume width; S, maximum bed slope, in brackets minimum bed slope; Active width, average value; h, average flow depth; U average flow velocity; Fr, Froude number; θ/θ_c, ratio of the Shields number to its critical value considering the bed surface grain diameter variation (i.e., the lower value of the range is θ/θ_c computed with the D_{84} of the coarse fraction, the upper limit of the range is θ/θ_c computed with the D_{84} of the fine fraction). $\theta = \frac{\tau}{\rho(s-1)gD_{84}}$ where $\tau = \rho ghS$ and $\theta_c = 0.06$ after Ashida and Michiue (1972).

flume width did act as a lateral constraint on active channel migration. The third experiment had a lower flume width corresponding to a confined flow. Run 3's flume width was set equal to the equilibrium active channel width (a common situation in the field, as illustrated in Figure 1) observed and documented during the previous experiments Runs 1 and 2; we interpreted such channel width as the width of the self-formed channel in equilibrium with the specific values of feeding rates, channel slope, and grain size distribution. We specify that this equilibrium width was an average value over the entire duration of the run, as the active width fluctuated, it "instantaneously" varied. Also the bed surface sediment composition, the bed slope and the bedload transport rate fluctuated, as is natural in dynamic equilibrium conditions.

2.2. Measurements and Data Acquisition

In each experiment we measured the sediment transport rate in terms of outlet sediment discharge. We measured it every 20 min by weighing the exiting sediments collected in buckets. This value was not an instantaneous value of the outlet sediment discharge, but a value averaged on the time interval of 20 min. We weighed sediments using a balance with a precision of 1 g.

Throughout all of the runs, we performed manual measurements on the bed morphology in three cross sections that were evenly spaced in the central part of the flume, located 1.7, 2.9, and 4.2 m from the inlet. Every 30 min, without interrupting the runs, we collected measurements of x, y, and z, thus measuring the bed elevation and the active channel width (when many branches were present a main active channel was always identified). Bed elevation was measured in several points evenly distributed throughout the cross section (also including points in the wetted areas and dry areas that were present in the unconfined flow configurations of Runs 1 and 2, hence the longitudinal gradient referred to the large alluvial bed rather than the active channel). Bed elevation was measured using a digital depth gauge with a precision of 0.1 mm. We inferred slope from bed elevation measurements. The slope fluctuated and we consider the maximum slope (Table 2) as the equilibrium slope. The three runs developed the same maximum slope, which is identified with the long-term equilibrium slope (Recking et al., 2009). As will be presented below, increasing the lateral constraint promotes vertical sorting which in turn increases bed (and slope) instabilities as was described by Recking et al. (2009).

For the entire duration of the runs and without interrupting the flow we carried out a photographic survey aimed at measuring bed surface sediment composition by processing images taken from above. We used a Canon 450D; the focal length was 24 mm; the horizontal resolution of the image as well as the vertical one was 72 dpi. The camera was equipped with a polarizing filter (HOYA cir-polarizing filter) able to reduce water reflections. The camera was placed 2.5 m above the central part of the flume, framing precisely the central 2.8 m of the flume length. Given the position of the camera together with its focal length, we had a ground pixel size of 1.26 mm. The camera shooting frequency was one photo per minute. Given that the two sediment fractions had different colors, we could process the photos through a code based on color detection providing the areal fraction content of a surface area covered by a certain color, that is, a certain grain size. The separation of coarse grains from fines could be achieved both at the grain scale (determining fractions' percentage) and then at the pattern scale. Indeed we could identify and isolate patches of coarse grains as well as patches of fines. These analyses at the pattern scale were achieved through morphological operations (Soille, 2013), as follows. The two sediment fractions captured in the photos had different colors, and thus different radiances in photos. Radiance is information stored in the photos' pixels. Pixels have values, called digital numbers (DN), which have a one-to-one correspondence with radiance. We analysed the DNs' histograms of coarse grains and fines in the three bands of the RGB photos captured during preliminary experiments. We found that in the blue channel fine grains and coarse grains have DNs' histograms with the minimum overlapping. We could therefore set a threshold on DNs' histograms in the blue channel and thus distinguish and separate coarse grains from fines. Figure 2 shows an example of an original RGB photo (Figure 2a), the thresholded binary image (Figure 2b), and the patch of fine sediments identified through morphological operations (Figure 2c). The accuracy evaluation of the operation of fractions' separation has been implemented on the threshold values. The evaluation of the accuracy of the operation of fractions detection consists in estimating the error occurring when detecting fractions by applying the specific thresholds we defined (Table 3). By applying a certain threshold value we identify as fine (coarse) grains all the pixels whose DN is lower (higher) than the threshold. However, as reported in Table 3, a few coarse grains actually have pixels' DN lower than the threshold and they are detected as fines (thus coarse

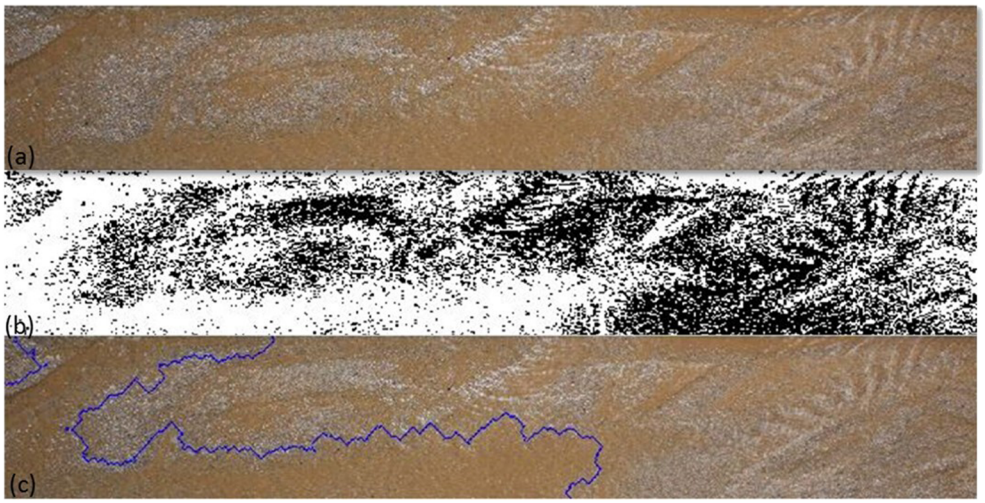

Figure 2. A photo taken during Run 1; the central 2.8 m of the flume length are framed, the flow is from left to right. Small-scale variations in the top right corner are not due to water surface waves. They correspond to alternate bands of coarse and fine sediments characterized by a topographic signature as well. The water surface is in phase with this bottom undulation since $Fr > 1$. (a) The original RGB photo; coarse grains are white (light gray) and fines are orange. (b) The binary image resulting from the thresholding; coarse grains are black and fines are white, the totality of white pixels are recorded to provide % Fine. (c) The delimitation of the detected zone of fines, this area provides % Area Fine (% Area Fine < % Fine).

grains erroneously detected as fines), and there are a few fine grains which actually have pixels' DN higher than the threshold (thus fine grains erroneously detected as coarse ones).

For the hydraulic characterization of the flow we measured for each run the flow depth and the flow velocity at points along several cross sections at specific times. In Runs 1 and 2, with low lateral confinement, we measured the flow depth, the flow width, and the flow velocity where the flow actually took place; that is, the hydraulic measurements were limited to the active channel (i.e., no measurements in the emerged areas). The flow depth was measured using a digital depth gauge; the flow velocity was measured through large scale particle image velocimetry (Fujita et al., 1998; Le Coz et al., 2014; Piton et al., 2018), and the mean flow velocity was obtained from the 2-D surface velocity field.

At the end of each run we took samples of the substrate. For each run we took about 10 samples evenly distributed along the flume obtained by removing a 5-mm-thick superficial sediment layer. The spacing and the $x - y$ dimensions of the samples were about 40 cm and 5 by 5 cm, respectively. The samples were dried and sieved and then the substrate sediment composition determined (volume fraction content).

2.3. A Proxy for the Active Channel Width

Among the image processing operations for determining the bed surface texture, the operation of identifying patches of fine sediments is particularly important because we could associate the area covered by patches of fines to the measurements of the active channel width. For all the images captured for the analysis of the bed surface sediment composition, (i) we detected the patches of fines, (ii) we determined their areal extent, (iii) we summed the total area occupied by patches of fines, (iv) we expressed the latter as the percentage

Table 3
Run Specific Threshold and Error Quantification for Sediment Separation Analysis

Run #	Threshold value on pixels' DN	Error on fine grains (%)	Error on coarse grains (%)	Overall error (%)
1	100	0.45	6.8	5.12
2	95	2.15	3.35	2.78
3	96	0.74	2.9	1.91

Note. Errors are expressed in percentage since they are quantified as the ratio between pixels erroneously detected and the total amount of pixels; this ratio is both fraction-specific (error on fine grains, error on coarse grains) and for the sum of the two fractions (overall error).

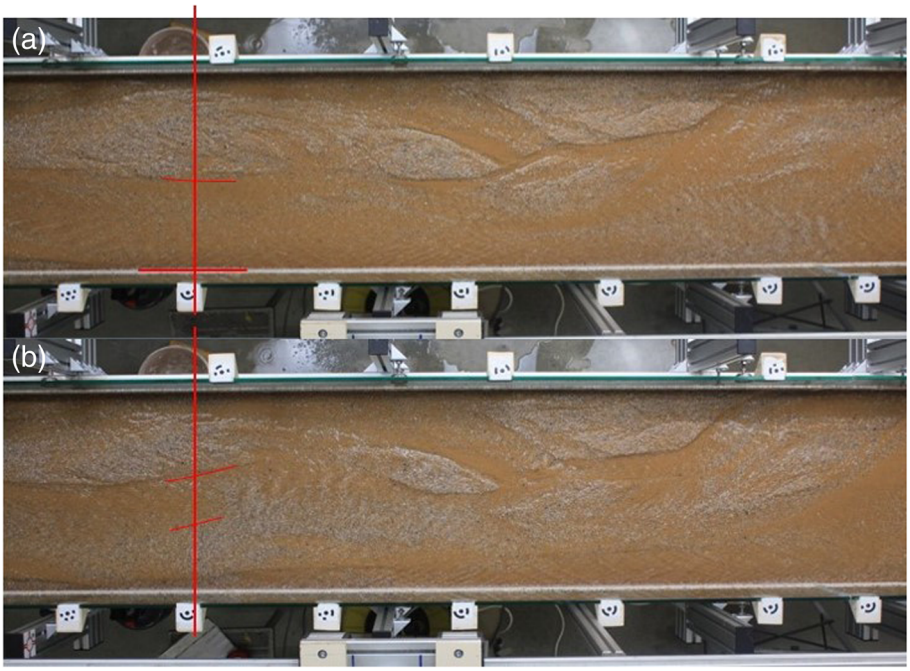

Figure 3. Photos taken during Run 1; the central part of the flume is framed (2.8 m of the flume length), the flow is from left to right. The red line indicates a section where we measured the main active channel width; emerged zones are mainly composed by patches of coarse grains (light gray). (a) instant: 29 hr and 29 min: the channel, on the right side covers half width on the flume; the active channel bed is composed of fines (orange). (b) instant: 29 hr and 36 min: the main active channel is narrower, concomitantly a greater amount of coarse-grained sediment covers the flume bed.

of the total framed area, and we labeled this value % Area Fine. Instead, the term % Fine indicates the percentage of the fine fraction covering the bed surface: % Fine is the information of how many grains are fine grains, and it does not take into account if fine grains are aggregated or not. The difference between % Fine and % Area Fine is illustrated in Figure 2.

We observed that in our experiments intense transport always occurred over large patches of fines (orange sand in Figure 3); the bed of the active channel was mainly composed of fine sediments. The greater the extension of the zones rather homogeneously composed of fines, the larger was the main active channel width, and the more intense was the sediment transport. Hence, we could use the area covered by patches of fines as a proxy for the active channel width (Figure 3). The methodology we performed to assess active width may be added to the general relationship for predicting the active width from simple parameters that would be applicable over a range of river conditions (i.e., slope, discharge, and grain size) such as the predictors on active width proposed in Ashmore et al. (2011). We note that direct measurement of the active channel width represents a local measurement, carried out at given cross sections, whereas the area covered by patches of fines concerns a region. Therefore, the assessment of the active channel width through the area covered by patches of fines represents a choice in favor of reach-scale rather than local cross-sectional parameters. This choice is consistent with recommendations by Peirce et al. (2018) who proposed "that research in complex gravel-bed rivers consider investigating reach-scale morphodynamic parameters and thresholds, which might be more meaningful, and more efficient, in terms of understanding overall channel change and bedload transport rates than thresholds strictly focused on grain-scale dynamics."

3. Results and Analysis

3.1. Channel and Planform Morphology

The experimental observations on the three runs confirmed the experimental results by Garcia Lugo et al. (2015) on the morphological changes induced by variations of the channel lateral confinement. As in Garcia Lugo et al. (2015), we observed that changing only the lateral confinement resulted in bed morphology and complexity that varied greatly (Figure 4).

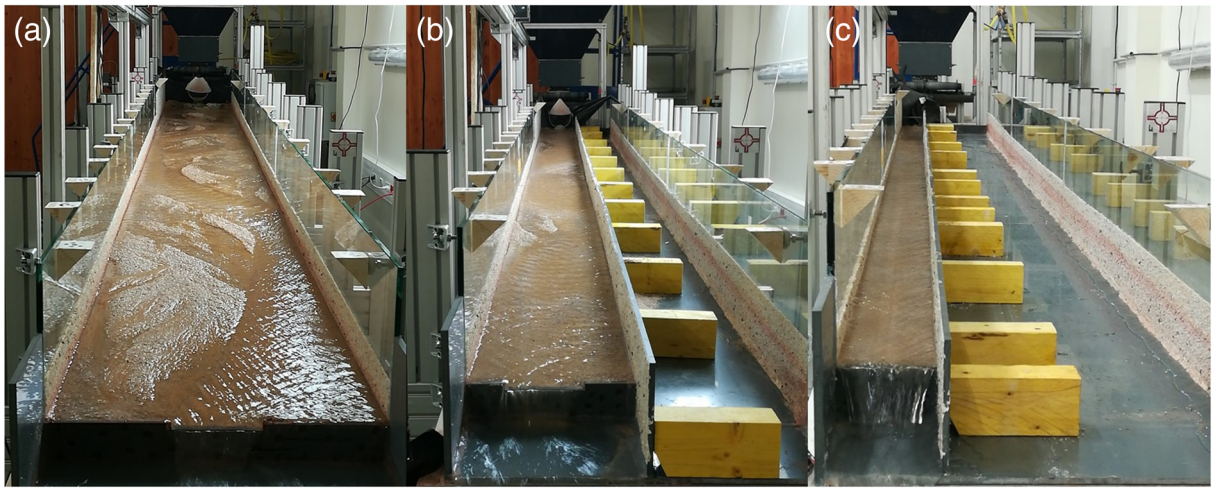

Figure 4. The three runs configurations. (a) Run 1, flume width 0.5 m. (b) Run 2, flume width 0.25 m. (c) Run 3, flume width 0.12 m.

Run 1 was characterized by a braided pattern in which the bed system exhibited rapid changes in the main channel planform configuration accompanied by sorting processes. The multithreaded channel wandered in the large alluvial bed, rapidly forming and destroying multiple bars and producing on the bed surface well-defined patches of coarse sediments and fines. This continuous and rapid evolution and rearrangement of the bed surface had a fast pace of 1–5 min. In the braided pattern of Run 1 we could always identify a main active channel, thus confirming literature on laboratory and field observations that indicate that a large proportion of the channel flow (up to 95%) can be conveyed by a single anabranch (Egozi & Ashmore, 2009; Peirce et al., 2018). The intermediate width of Run 2's configuration produced a morphology of central/multiple bars. Indeed Run 2 was characterized by the presence of a wandering channel, where the term wandering is used to denote a channel with a transitional morphology between single thread and braiding, according to the classification by Church (1983) and Church (2006). The third experiment had the configuration with the highest lateral constraint (Table 2 and F igure 4c) producing a confined channel morphology. In this configuration the width-to-depth ratio was such that not even alternate bars could form.

3.2. Grain Sorting

The experimental observations on the three runs revealed that variations of the channel lateral confinement led to substantial changes in sorting processes and patterns. Sorting processes and patterns occurred with different intensity, in different directions (planimetric versus vertical sorting), and different spatial scales depending on the lateral flow constraint. In particular, the degree of lateral confinement determines how surface sorting occurred: longitudinal sorting only or both longitudinal and lateral sorting.

Both in Runs 1 and 2 substrate samples taken at the end of the run had the same composition of the initial bed mixture (feeding sediment mixture, see section 2.2); precisely the substrate samples composition differed from the mixture (60% coarse, 40% fines) of ±2–3.

Granular physics tell us that when the sediments of a mixture are transported together, they necessarily interact, through sorting processes (Bacchi et al., 2014; Frey & Church, 2009). Sorting can occur in the horizontal plane, or in the vertical, with a relative importance which is expected to depend on the degree of freedom allowed by the channel. Both in Runs 1 and 2 the granulometric sorting of the bed surface, namely planimetric sorting, markedly occurred both in the streamwise and in the spanwise directions. This surface sorting consisted in clearly detectable patches of coarse sediments and patches of fines, both mobile and both characterized by a rapid dynamic. In Run 3 surface sorting was intense and acted only longitudinally. In this highly confined flow configuration the flow was able to act only in the longitudinal direction and no transversal bed states variations such as lateral sorting occurred. Then, we could state that sorting patterns took place in a plane only in presence of lateral space as in less confined flow configurations of Runs 1 and 2. With respect to Runs 1 and 2, the sorting patterns of Run 3 were more homogeneous (coarse patch with less intrusions of fines and vice versa) and they were also much longer (Figure 5). Without the degree of freedom consisting in transversal bed state variations, substantial sorting processes could affect larger spatial scales:

Figure 5. Extended sorting patterns characterizing some bed stages of Run 3; the central 2.8 m of the flume length are framed, the flow is from left to right. (a) A coarse-grained bed state, instant: 15 hr, 29 min. (b) A fine-grained bed state, instant: 15 h, 37 min.

longer reaches with respect to patches of Runs 1 and 2. In Run 3 the flow regained a degree of freedom provoking vertical sorting processes, which are instead negligible in conditions of low lateral confinement. Furthermore, in Run 3 we also observed the formation of bedload sheets (similar to Recking et al., 2009), a peculiar phenomenon of longitudinal sediment sorting (Colombini & Carbonari, 2020; Iseya & Ikeda, 1987).

Therefore, despite using the same material, grain sorting led to very different situations with confined and unconfined flows. For Runs 1 and 2, the flow and transport could easily bypass any local blockage due to patches of poorly mobile coarse sand. In the case of Run 3, obviously such bypass was not possible anymore and local blockage could propagate over very long distances, leading to bed armoring (and promoting a vertical sorting with the coarse fraction at the surface and the fine fraction in the subsurface) instead of a lateral sorting as was the case in Runs 1 and 2 (compare, for instance, Figures 5 and 3). The difference in patchiness between Runs 1 and 3 can be related to field conditions, such as the example shown for the Séveraisse river in Figure 1. A reach of the Séveraisse river exhibits an upstream braided part where channels' adjustments take place in the plane, and bed surface grain sorting is relevant (D_{50} = 37 mm, D_{84} = 113 mm) also presenting patches of coarse grains and patches of fines. Instead, in the downstream part the channel is confined and adjustments only take place in the vertical direction; a strong armoring is present (D_{50} = 110 mm, D_{84} = 303 mm). Multiple bars, patches of coarse sediments, and patches of fines of Run 1, as those in Figure 3, are analogous to the morphological characteristics of the upstream braided reach of the Séveraisse; surface coarsening as in some bed states of Run 3, Figure 5a, is analogous to the downstream confined reach of the Séveraisse. Our flume observations are also consistent with the field observations by Mueller and Pitlick (2014) on bed coarsening in single thread reaches compared to weakly armored braided reaches.

Table 4
% Coarse of the Bed Surface for Runs 1, 2, and 3

		Run 1	Run 2	Run 3
% coarse	average	25.5	21.2	19.5
	median	25.2	19.8	17.7
	variance	28.5	77.5	92.7
	25th percentile	21.9	14.8	12.7
	75th percentile	28.6	26.0	24.1
	min	11.7	2.0	4.6
	max	47.4	61.1	75.2
	range	35.8	59.1	70.5
	coefficient of variation	0.2	0.4	0.5

Note. Instantaneous measurements from photos taken from above every minute.

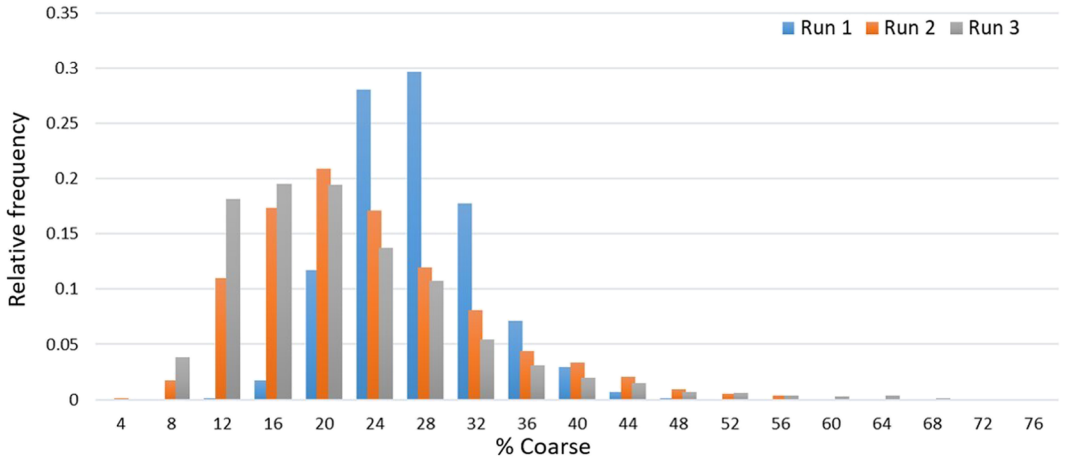

Figure 6. Frequency distribution of % Coarse values for Runs 1, 2, and 3.

3.3. Fluctuations of Surface Texture, Slope, and Transport Rate

Albeit the runs were conducted under constant feeding rate conditions, in all the runs the components of channel dynamics and bedload transport varied significantly and continuously. We observed significant fluctuations of the percentage of the granulometric fractions composing the surface texture (Table 4, Figure 6). Also the bed slope oscillated in all the three different flow confinement configurations (Table 5, Figure 7). Fluctuations of bed slope occurred essentially through an alternation of aggrading and degrading bed states. Given that the outlet section had a fixed bed elevation, overall aggradation corresponded to an increase of bed slope, whereas overall degradation corresponded to a decrease in bed slope. In all the runs, the outlet sediment discharge (Table 6) had an average value that almost equalled the constant value of the inlet sediment discharge (Table 2), thus the experiments met the dynamic equilibrium condition illustrated at the beginning of section 2. The outlet sediment discharge presented continuous relevant fluctuations over time around the average value (Table 6, Figure 8). Such fluctuations have already been shown in other flume experiments (Bacchi et al., 2014; Recking et al., 2009) even if with a different lateral confinement, precisely in narrow flume configurations. Among the basic indicators and descriptive statistics reported in Tables 4, 5, and 6 we also introduced a standardized measure of dispersion of the data: the coefficient of variation defined as the ratio of the standard deviation to the mean and it represents the extent of the variability in relation to the mean. The coefficient of variation represents a comprehensive indicator for data variability. In section 3.5 we analyze how variability of surface texture, slope, and transport rate depends on flow lateral confinement, we hereby investigate how data variability changes in the three runs, whereas the next subsection illustrates surface texture, slope, and transport rate as time series with complex relationships.

Table 5
The Slope for Runs 1, 2, and 3

		Run 1	Run 2	Run 3
Slope (m/m)	average	0.0326	0.0286	0.0274
	median	0.0327	0.0285	0.0273
	variance	$7.94 \cdot 10^{-7}$	$1.33 \cdot 10^{-6}$	$1.96 \cdot 10^{-6}$
	25th percentile	0.0317	0.0277	0.0265
	75th percentile	0.0328	0.0292	0.0282
	min	0.0306	0.0262	0.0246
	max	0.0342	0.0323	0.0318
	range	0.0036	0.0061	0.0073
	coefficient of variation	0.0270	0.0400	0.0510

Note. Instantaneous, manual measurements of the bed elevation taken every 30 min.

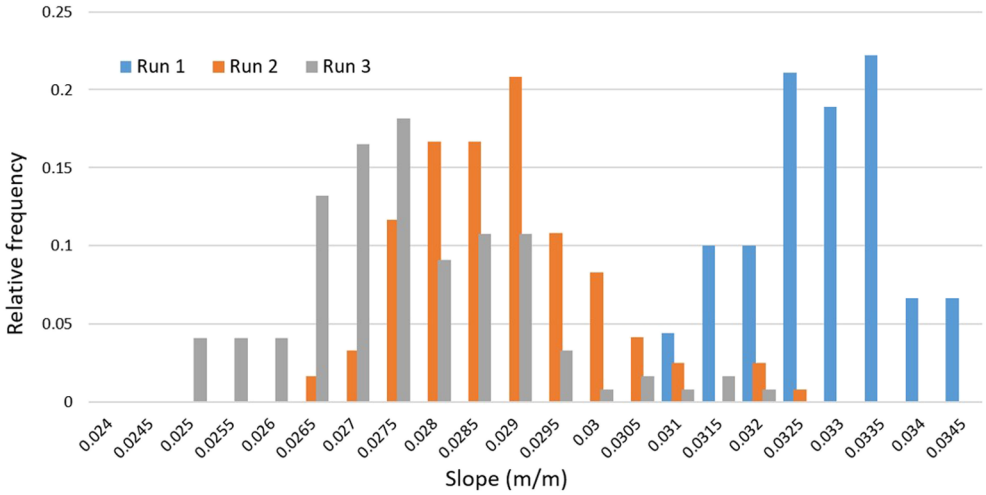

Figure 7. Frequency distribution of bed slope values for Runs 1, 2, and 3.

3.4. Coupling Channel Morphodynamics to Bedload Transport

Surface sediment composition, bed slope, and sediment transport rate have a complex mutual dependence. They vary with the morphodynamic evolution of the channel bed. Thanks to the continuous monitoring of surface sediment composition, bed slope, and sediment transport rate, we obtained continuous signals of these variables and we could establish trends and feedbacks between such signals.

All three runs presented a similar relationship between the bed surface sediment composition, the bed slope, and the sediment transport rate. Such feedback is reported in Figure 9 concerning the outcomes of Run 1. Figure 9 shows the temporal evolution of bedload transport rate, slope, and surface sediment composition; for the latter, all three signals are reported % Coarse, % Fine, and % Area Fine. The difference between % Fine and % Area Fine has been illustrated in section 2.3. The evolution over time of the percentage of the coarse fraction was in opposition with the temporal evolution of the sum of the surfaces covered by patches of fines (Figure 9a): when the percentage of the coarse fraction increased, the area covered by patches of fines decreased and vice versa. In all circumstances the unconfined bed produced patches of fines (zones of active transport). However, the general pattern suggests that patches decreased during aggrading phases (e.g., 33- to 38-hr time window) and increased during degrading phases (e.g., 15- to 20-hr and 38- to 47-hr time windows). In Figure 9, the 15- to 20-hr time window characterized by a wide area of patches of fines, low slope values, and an increase of sediment discharge is highlighted by black dashed lines, whereas gray dashed lines highlight the 33- to 38-hr time interval during which the area covered by patches of fines is

Table 6
The Outlet Sediment Discharge for Runs 1, 2, and 3; 20 min Average Measurements[a]

		Run 1	Run 2	Run 3
Q_s (g/s)	average	7.64	8.04	7.47
	median	7.64	8.01	7.48
	variance	1.94	1.24	1.75
	25th percentile	6.68	7.22	6.82
	75th percentile	8.47	8.65	8.21
	min	4.42	5.74	2.41
	max	12.40	12.09	13.52
	range	7.98	6.35	11.11
	coefficient of variation	0.18	0.14	0.18

[a]The indicators have all the same unit of $Q_{s,out}$, g/s, except the variance, g^2/s^2, and the coefficient of variation, (_).

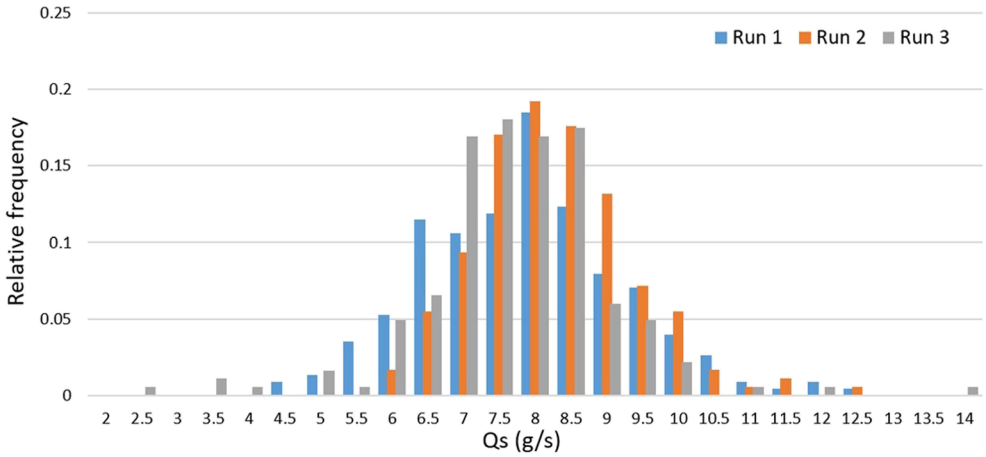

Figure 8. Frequency distribution of outlet sediment discharge values for Runs 1, 2, and 3.

small, bed slope has high values, and the sediment discharge is decreasing. The feedback between the slope and the sediment discharge can be described as follows: During phases of increasing bed slope, we registered minimum values of the outlet sediment discharge resulting in aggradation and low grain mobility, whereas just after the bed slope reached the maximum value equal to about 3.4% for Run 1, we registered high values in the outlet sediment discharge associated with a high grain mobility. Subsequently, we measured an upper-middle, ~8–10 g/s, sediment discharge at the outlet which lasted even when the bed slope had already decreased, meaning that the "bed system" needed some time to evacuate sediments previously stored. The % Area Fine signal and the Q_s signal had a comparable pattern with a lag of the latter with respect to the former (Figure 10). After the maximum bed slope was reached, the coarse pavement (relatively wide) was suddenly destroyed, resulting in a decrease of the coarse percentage and an increase of the fine patches accompanied by erosion episodes which led to high values of sediment discharge registered in the outlet section with a lag time due to damping effect of the flumes wide lateral space.

The same feedbacks and the same bed states were observed also in the more confined configurations of Runs 2 and 3: stages of aggradation and overall deposition accompanied by surface coarsening and low grain mobility alternating with stages of degradation and overall erosion accompanied by bed surface fining. Figure 11 shows the trend of sediment discharge, slope, and surface fractions' composition of Run 3. The plot

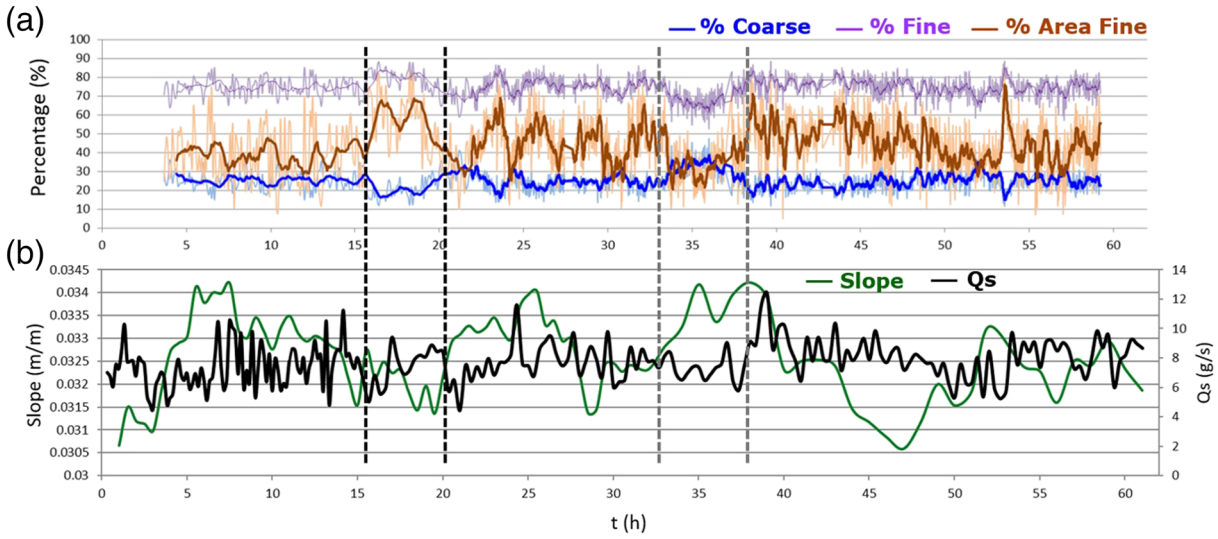

Figure 9. Run 1. (a) Time series of the percentage of the coarse fraction of the bed surface, the fine fraction of the bed surface, and the total surface covered by patches of fines; simple moving average (SMA) of each quantity is shown as well. (b) Time series of the average bed slope and the outlet sediment discharge. Measurements of slope and surface sediment compositions are instantaneous, whereas sediment discharge is a 20-min average measurement.

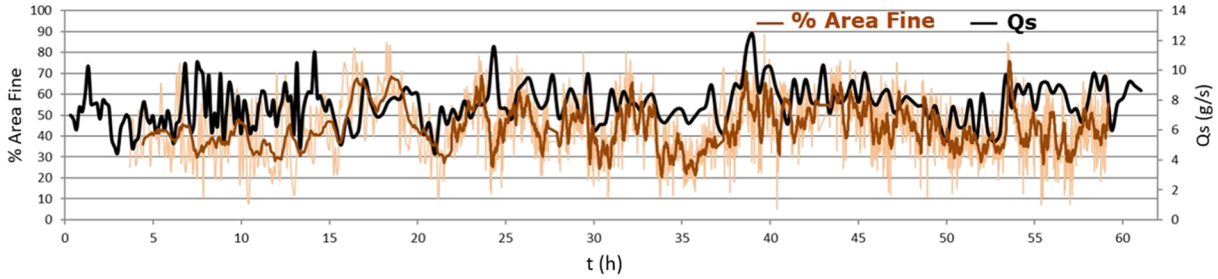

Figure 10. Run 1. Time series of the outlet sediment discharge and the total surface covered by patches of fines. Measurement of the total surface covered by patches of fines is instantaneous, whereas sediment discharge is a 20-min average measurement.

of the sediment discharge and the slope together (Figure 11a) reveals that the two signals had the same trend with a slight lag of Q_s with respect to the slope. Rising parts of the slope signal were followed by rising parts of the Q_s signal, and falling limbs of the slope signal were followed by falling limbs of the Q_s signal. Figure 11 shows that the narrower the flow configuration, the less relevant is the lag time between the different signals indicating that the lag time is due to the damping effect of the flume's wide lateral space. Aggrading bed was associated with low outlet sediment discharge and aggrading stages went together with coarsening stages of the bed (Figure 11c). This behavior was particularly evident and intense in the time windows near hours 15 and 30, where slope peaks near the maximum value of 0.032 (Figure 11). Actually, at these moments of the run we observed trains of bedload sheets, as defined in Whiting et al. (1988) and Venditti et al. (2008). Trains of bedload sheets resulted in an efficient process of bed coarsening, as described in Recking et al. (2009). This stage of rapid and intense aggradation and coarsening stopped with the attainment of a maximum slope (Figure 5a); then a sharp rapid erosion took place in conjunction with bed fining (Figure 5b) and a peak of outlet sediment discharge. These bed stages confirmed the experimental observations by Recking et al. (2009) who described sediment pulses associated to bedload sheets migration.

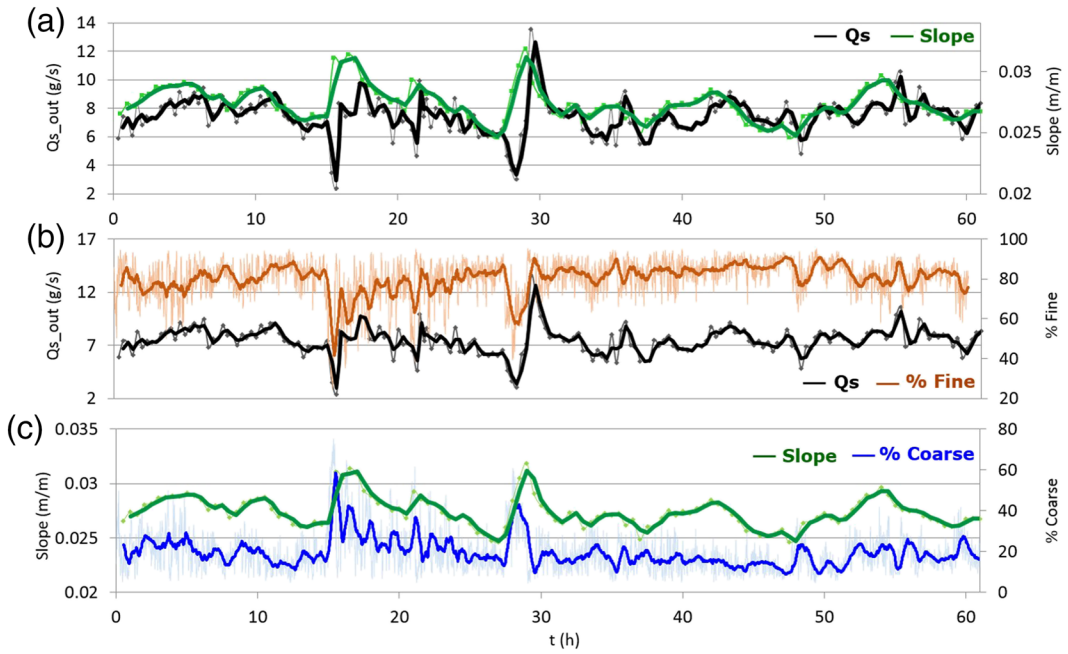

Figure 11. Run 3. (a) The sediment discharge and the slope signals. (b) The slope and the % Coarse signals. (c) The sediment discharge and the % Fine signals. Both the signals themselves and their simple moving average (SMA) are plotted. Measurements of slope and surface sediment compositions are instantaneous, whereas sediment discharge is a 20-min average measurement.

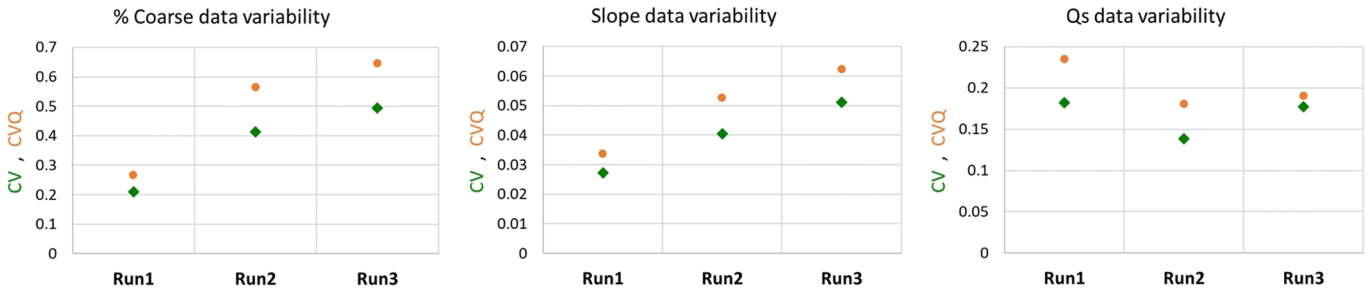

Figure 12. (left) % Coarse, (middle) slope, and (right) Q_s data variability for Runs 1, 2, and 3. In green the coefficient of variation, CV; in orange the coefficient of quartile variation, CQV. The CQV is considered a robust estimator of the CV (Ospina & Marmolejo-Ramos, 2019).

3.5. Analysis of Variability of Surface Texture, Slope, and Transport Rate in Different Flow Conditions

All the runs presented significant fluctuations of the bed system signals (% Coarse, its dual % Fine, % Area Fine, Slope, $Q_{s,\,out}$); however, the amplitude and the main statistical features of such fluctuations varied from one run to another (section 3.3), in other words the degree of data variability depends on the degree of flow lateral confinement. In the following analysis of data variability, we validated the information provided by the classic coefficient of variation using the coefficient of quartile variation defined as the ratio between the interquartile range (25th–75th percentiles) and the median, and considered a robust estimator of the coefficient of variation (Ospina & Marmolejo-Ramos, 2019).

Variability of the coarse fraction composing the bed surface deserves particular attention in light of the above analysis on grain sorting (section 3.2). The values of % Coarse presented a higher variability in Run 3 with respect to Runs 1 and 2: variance, coefficient of variation, and coefficient of quartile variation of Run 3 were higher than those of Runs 1 and 2. This is because % Coarse reached high values when coarse grains covered a long reach of the flume (Figure 5a), whereas the minimum values of % Coarse corresponded to bed states of fining on a long reach (Figure 5b). Conversely, in Runs 1 and 2 lateral sorting caused surface patchiness with shorter spatial scales, and in the area framed for the analysis of surface texture patches of coarse grains and patches of fines always coexisted, thus the percentage of a single size fraction did not reach the extreme values characteristic of Run 3. Overall, % Coarse data (Table 4 and Figure 6) present a trend of increasing variability from Runs 1 to 3. This trend is well represented by the coefficient of variation, plotted in Figure 12, as well as by the frequency distribution (Figure 6) showing that Run 1 has a higher degree of concentration of frequencies with respect to Runs 2 and 3. In other words, from Run 1 to Run 3 the frequency distribution is less and less peaked, thus revealing an increase in % Coarse data dispersion. The same trend of increasing variability characterized the slope signal (Table 5): from Run 1 to Run 3 the slope signal is characterized by a relevant increase of the range, the variance, and the coefficient of variation (with its estimator the coefficient of quartile variation). Also, the frequency distribution of the slope values (Figure 7) reveals an increasing slope data dispersion from Runs 1 to 3. Run 3 showed the highest variability of the slope signal, being the experiment with the most intense and efficient aggradation and degradation process: The bed elevation increased and decreased significantly, corresponding to a vertical bed "breathing". The signal of the outlet sediment discharge, reported in Table 6, presented a different behavior with respect to the % Coarse and slope data: The variance and the coefficient of variation (Table 6) do not present an increasing trend from Runs 1 to 3. Precisely, the coefficient of variation of the signal $Q_{s,\,out}$, as well as the coefficient of quartile variation, has a minimum in the case of Run 2, as represented in Figure 12, while the frequency distribution of the transport rate values of Run 2 is slightly more concentrated with respect to those of Runs 1 and 3 (Figure 8). We interpret the variation in Q_s as the storage and release of sediments, which varies due to how lateral flow constraints affect bedload transport; we address this issue in the next section.

4. Discussion

4.1. Sediment Storage, Transfer, and Release

The variability of the Q_s data is connected to the process of storage and release of sediments: when the outlet sediment discharge has a high variability (the Q_s coefficient of variation has a high value) the process of storage and release of sediments is relevant, either for the high frequency of deposit formation and erosion,

or for the significant volume of sediments involved in the process. If the bed is in conditions that promote storage of sediments then release after a while, the system encounters conditions of intermittent sediment transfer, or at least a sediment transfer that exhibits great changes in terms of magnitude and occurrence. On the contrary, when Q_s has a low variability the process of storage and release is less important, whereas the sediment transfer has an optimum, meaning a less variable behavior in time (optimum in the sense of minimum Q_s variability). In other words, in this second case the bed has not relevant stocks of sediments cyclically formed and destroyed by the flow, and thus the channel is not affected by relevant discontinuous input of sediments, the channel rather presents an actual "flume-like" behavior transferring downstream a sediment discharge not highly varying in terms of magnitude and occurrence. An optimum sediment transfer is associated with a minimum storage and release process.

Runs 1 and 3 were characterized by a high variability of Q_s and by an efficient process of storage and release. However, this effective storage and release process took place in different ways and with different features in these two experiments. The significant storage and release process in Run 3 was characterized by an "altimetric functioning" (vertical exchange): The formation and destruction of sediments stocks occurred with altimetric variations and without cross-channel variations. Evidences of this "vertical breathing" were as follows: the most intense and efficient aggradation and degradation process; the highest variability of slope; the most intense and efficient coarsening and fining of the bed surface (the first associated with aggradation and the second associated with degradation, respectively); and the substrate samples which proved the presence of vertical sorting. The relevant storage and release process occurring in Run 1 took place in a very different, even opposite, way that we labeled "planimetric functioning." In this wide, unconfined flow configuration no vertical sorting took place; the variability of the bed slope was the lowest with respect to the other experiments; and above all, a large lateral space let the main channel wander and build, destroy, and rebuild depositional patterns.

In Run 2 the process of storage and release of sediments was not efficient nor particularly relevant since there was neither a strong altimetric functioning, nor a strong planimetric one. With respect to Runs 1 and 3, Run 2 is the test in our set of experiments where the lateral constraint and the flow width implied the minimum storage and release of sediments which corresponded to an optimum downstream sediment transfer. In other words, with respect to Runs 1 and 3, Run 2 was the configuration in which the main channel was the most efficient from a sediment transfer point of view; the channel conveyed sediments at the outlet section with the most "flume-like" behavior, namely the minimum relative Q_s fluctuations.

4.2. Toward a Channel Morphology for Optimal Sediment Transfer

We now extend the obtained results through further consideration and by speculating about the morphology that transfers the sediments downstream in the most regular way, that is, not having a channel bed with periodic substantial storage of sediments, but rather having a bed with less varying channel characteristics (namely a minimum storage and release of sediments).

We assumed that a single-thread channel with alternate bars represents a morphology stable and suitable to convey sediments downstream in the least fluctuating way. For this to happen it seems reasonable to consider a single-thread channel, because otherwise in a multithread channel with abundant medial bars, such as in Run 1, channels build and wipe away sediment deposits, thus making the sediment transport rate highly fluctuating. On the other hand, in a confined single-thread channel (i.e., a channel with a width-to-depth smaller than the critical value for alternate bars' formation as our Run 3, indeed a flat bed configuration) the altimetric variations of the bed are very relevant, and thus in this case too the sediment transfer is highly fluctuating. Actually, our set of experiments did not include an alternate bar configuration, which would have been achieved, maintaining the water discharge, the flume slope, and the sediment mixture set for the whole ensemble of our runs, by reproducing an intermediate flume width with respect to Runs 2 and 3. Classical theory of bars morphodynamics (Colombini et al., 1987) provides, for a given water discharge, channel slope, and median grain size, the critical value of the width-to-depth ratio for bar formation. We applied bar formation theory to our experimental conditions in order to verify through analytical modeling the channel morphologies observed in the flume. The analysis was implemented using an open source tool named TREMTO (Theoretical RivEr Morphodynamics TOol) developed by the researchers of the University of Trento and based on the Colombini et al. (1987) analysis. It turned out that Run 2 had a width-to-depth ratio more than 4 times greater than the critical value for alternate bar formation: The analysis suggested that in Run 2's wide configuration central/multiple bars would occur. Conversely, Run 3 had a width-to-depth

ratio slightly smaller (about 8%) than the critical value for alternate bar formation: Run 3's narrow configuration corresponded to flat bed (no bars) conditions. Hence, we confirmed that our runs configurations did not reproduce a strictly alternate bar configuration, the configuration we suppose to be the most efficient in downstream sediment transfer having a less varying channel morphology which can convey the sediment discharge with limited fluctuations with respect to wider and narrower flow configurations.

Francalanci et al. (2012) and Peirce et al. (2018) analyzed sediment transport depending on the morphology where it takes place. They provided analyses that can be linked to the concept of optimum sediment transfer and minimum storage and release applied to a bar regime, as proposed in the present contribution. As illustrated in section 1, Francalanci et al. (2012) compared sediment transport in a 3-D numerical model with well-developed alternate bars and sediment transport in an equivalent 1-D case of flat bed (equivalent in terms of macroscopic roughness, slope, and mean velocity) and they concluded that alternate bars strongly enhance bedload transport at low Shields stress, that is, the bedload transport rate is greater. We found this outcome in accordance with our speculation about optimum sediment transfer characterizing the alternate bar morphology among all the other morphologies typical of gravel bed rivers. Indeed, optimum sediment transfer can be interpreted either way: considering the magnitude of the sediment transport rate (Francalanci et al., 2012) or considering fluctuations and possible intermittency of the sediment transport rate (as we suggested). Peirce et al. (2018) analyzed bedload transport rate exactly in that sense: They focused on the variability of the bedload transport rate rather than on its magnitude, its intensity. Peirce et al. (2018) performed five constant-discharge experiments in a range of flume conditions typical of gravel bed rivers. The authors' main objective was the analysis on the variability of the active width above all in braided channels; however, they also analyzed bedload transport rate and they reproduced not only multithread channel configuration (experiments 4, 9, 12, and 13) but also a single-thread channel configuration characterized by the presence of alternate bars (Experiment 1). The experimental results by Peirce et al. (2018) showed that the single-thread channel with alternate bars presented the bedload transport rate with the lowest range of values (see Figure 9 in Peirce et al., 2018), i.e., the lowest variability compared to the variability of the transport rate characterizing the braided patterns. The authors stated that Experiment 1 seems to have a greater bedload transport rate than would be expected for the range of active widths (see Figure 10 in Peirce et al., 2018) and they assumed that the reason is a difference in the mode of transport such that bedload is less involved in dynamically developing morphology and therefore behaves more like a simple, plane-bed flume (Church, 2006; Recking et al., 2016).

The present contribution shows that braided channel, on one hand, and single-thread channel with high lateral constriction, on the other, present a highly fluctuating downstream sediment transfer associated with relevant bed adjustments and variations; we also propose that the alternate bars configuration is the gravel-bed rivers' morphology characterized by a less fluctuating sediment transport rate due to a channel minimizing the stock and release of sediment, an argument in line with the results and analyses by Francalanci et al. (2012), Recking et al. (2016), and Peirce et al. (2018). Furthermore, the present contribution relates the mechanism of storage and release of sediment to vertical and planimetric sorting occurring in the channel bed. Thus, sediment transport is analyzed depending on both channel morphology and mobile sorting patterns; we illustrated that the latter have a key role in sediment transport variability, showing that when sorting process are relevant (substantial surface fining and coarsening with vertical sorting, or relevant cross-section variability in granulometry) sediment transport is more fluctuating.

5. Conclusions

This set of experiments provided results on the effect of changing flume width on bed morphology, patterns of sorted sediments, and bedload transport rate.

This experimental activity showed that changes in the degree of flow lateral confinement have relevant impacts on bed morphologies. Increasing the river width implies an increase in bed complexity and thus the consequent improvement of riverine habitat and ecological quality. However, differences in lateral flow confinement resulted in the same average channel width (Runs 1 and 2). This confirmed the relevance of the active channel width when dealing with low confined gravel-bed rivers morphodynamics. Furthermore, the present contribution provided a method through image analysis of downward-looking photos by which we obtained a proxy for the active channel width represented by the area of the bed covered by patches of fine sediments. In particular, we implemented a new, simple, and high-resolution image analysis technique for

measuring the bed surface sediment composition, allowing to compute areal fraction content and to detect patches in a fully automated and nonintrusive fashion.

We provided for the first time an accurate monitoring of the bed surface sediment composition at different channel width constraints, showing that the latter strongly affect vertical and surface sorting patterns. In particular, vertical sorting did not take place in the low confined flow configurations of Runs 1 and 2 corresponding to central and multiple raw bars: The substrate samples, underneath a 5-mm-thick superficial sediment layer, had almost the same sediment composition of the mixture supplied (60% coarse, 40% fines; ±2–3% and ±3–4% for Runs 1 and 2, respectively). On the contrary, in highly confined flows with a width-to-depth ratio lower than the critical value for alternate bar formation, such as Run 3, vertical sorting substantially occurred: Substrate samples composition differed from the mixture (60% coarse, 40% fines) of about ±25%. Planimetric sorting occurred in all the flow configurations tested; however, in low confined flow configurations it occurred both in the streamwise and in the spanwise directions, whereas in highly confined flows bed surface sorting occurred only in the streamwise direction. Furthermore, patterns of sorted sediments were much longer in highly confined flows with respect to low confined ones. Hence, river lateral confinement has a primary control on the occurrence of vertical sorting and on the spatial scales of bed surface patterns of sorted sediments. Given that sorting patterns have a direct effect on bedload transport rate, this is a key point since in river management a very common action is to modify the river width and we showed that this modifies sorting characteristics and transport rates.

Lateral flow confinement has, therefore, an effect on bedload transport rate, precisely in terms of variability (magnitude and frequency of fluctuations). We measured an amplitude of the fluctuations of the bedload transport rate of 8, 6.4, and 11.1 g/s, for Runs 1–3, respectively; whereas the variance was 1.9, 1.2, and 1.8 g^2/s^2 and the ensuing coefficient of variation was 0.18, 0.14, and 0.18 for Runs 1–3, respectively. The values of the coefficient of variation were confirmed by those of the coefficient of quartile variation. Thus, the comparison of the three different flow configurations allowed us to identify, among the experiments carried out, what are the river morphologies characterized by a greatly varying downstream sediment transfer and what are those characterized by a more constant sediment transfer. We connected sediment transport variability to the process of storage and release of sediments, also by including for the first time the effect of sorting in the mechanism of storage and release of sediments. Finally, we extended this argument by assuming that among all the morphologies typical of gravel-bed rivers, the single-thread channel with alternate bars is the one characterized by a river bed with minimum storage and release of sediments and an optimum downstream sediment transfer.

Data Availability Statement

The data supporting the results and analyses of this research are available in the repository (10.5281/zenodo.3567673).

Acknowledgments
The Editor and three anonymous reviewers are thanked for their comments and suggestion, which substantially improved the manuscript. This research was supported by a doctoral grant provided by the University of Florence to C. Carbonari. Flume construction was supported by the French National Institute for Agriculture, Food and Environment (Inrae) centered in Grenoble. The Inrae Grenoble Centre also provided additional technical support and equipment during the experiments, and the technical staff of the institute is thus greatly acknowledged.

References

Ashida, K., & Michiue, M. (1972). Study on hydraulic resistance and bed-load transport rate in alluvial streams. *Proceedings of the Japan Society of Civil Engineers*, *1972*(206), 59–69.

Ashmore, P., Bertoldi, W., & Tobias Gardner, J. (2011). Active width of gravel-bed braided rivers. *Earth Surface Processes and Landforms*, *36*(11), 1510–1521.

Bacchi, V., Recking, A., Eckert, N., Frey, P., Piton, G., & Naaim, M. (2014). The effects of kinetic sorting on sediment mobility on steep slopes. *Earth Surface Processes and Landforms*, *39*(8), 1075–1086.

Bagnold, R. A. (1977). Bed load transport by natural rivers. *Water Resources Research*, *13*(2), 303–312.

Bagnold, R. A. (1980). An empirical correlation of bedload transport rates in flumes and natural rivers. *Proceedings of the Royal Society of London. A. Mathematical and Physical Sciences*, *372*(1751), 453–473.

Carson, M. A., & Griffiths, G. A. (1987). Bedload transport in gravel channels. *Journal of Hydrology (New Zealand)*, *26*(1), 1–151.

Church, M. (1983). Pattern of instability in a wandering gravel bed channel, *Modern and ancient fluvial systems* (pp. 169–180). John Wiley & Sons, Ltd.

Church, M. (2006). Bed material transport and the morphology of alluvial river channels. *Annual Review of Earth and Planetary Sciences*, *34*, 325–354.

Church, M. (2010). Mountains and montane channels, *Sediment cascades: An integrated approach* (pp. 17–53). Wiley-Blackwell.

Colombini, M., & Carbonari, C. (2020). Sorting and bed waves in unidirectional shallow-water flows. *Journal of Fluid Mechanics*, *885*.

Colombini, M., Seminara, G., & Tubino, M. (1987). Finite-amplitude alternate bars. *Journal of Fluid Mechanics*, *181*, 213–232.

Cudden, J. R., & Hoey, T. B. (2003). The causes of bedload pulses in a gravel channel: The implications of bedload grain-size distributions. *Earth Surface Processes and Landforms*, *28*(13), 1411–1428.

Dhont, B. (2017). Sediment pulses in a gravel-bed flume with alternate bars (Ph.D. Thesis).

Dhont, B., & Ancey, C. (2018). Are bedload transport pulses in gravel bed rivers created by bar migration or sediment waves? *Geophysical Research Letters*, *45*, 5501–5508. https://doi.org/10.1029/2018GL077792

Egozi, R., & Ashmore, P. (2009). Experimental analysis of braided channel pattern response to increased discharge. *Journal of Geophysical Research*, *114*, F02012. https://doi.org/10.1029/2008JF001099

Ferguson, R. I. (2003). The missing dimension: Effects of lateral variation on 1-D calculations of fluvial bedload transport. *Geomorphology*, *56*(1), 1–14.

Fienberg, K. S., Singh, A., Foufoula-Georgiou, E., Jerolmack, D., & Marr, J. D. G. (2010). *A theoretical framework for interpreting and quantifying the sampling time dependence of gravel bedload transport rates* (pp. 171–184). U.S. Geological Survey Scientific Investigations.

Francalanci, S., Solari, L., Toffolon, M., & Parker, G. (2012). Do alternate bars affect sediment transport and flow resistance in gravel-bed rivers? *Earth Surface Processes and Landforms*, *37*(8), 866–875.

Frey, P., & Church, M. (2009). How river beds move. *Science*, *325*(5947), 1509–1510.

Fujita, Y. (1989). Bar and channel formation in braided streams, *River meandering* (pp. 417–462). American Geophysical Union (AGU).

Fujita, I., Muste, M., & Kruger, A. (1998). Large-scale particle image velocimetry for flow analysis in hydraulic engineering applications. *Journal of Hydraulic Research*, *36*(3), 397–414.

Garcia Lugo, G. A., Bertoldi, W., Henshaw, A. J., & Gurnell, A. M. (2015). The effect of lateral confinement on gravel bed river morphology. *Water Resources Research*, *51*, 7145–7158. https://doi.org/10.1002/2015WR017081

Gomez, B., Naff, R. L., & Hubbell, D. W. (1989). Temporal variations in bedload transport rates associated with the migration of bedforms. *Earth Surface Processes and Landforms*, *14*(2), 135–156.

Henderson, F. M. (1966). *Open channel flow, Macmillan Series in Civil Engineering*. Macmillan.

Iseya, F., & Ikeda, H. (1987). Pulsations in bedload transport rates induced by a longitudinal sediment sorting: A flume study using sand and gravel mixtures. *Geografiska Annaler. Series A, Physical Geography, Vol. 69, No. 1 (1987), pp. 15-27 Published by: On behalf of the Wiley Swedish Society for Anthropology and Geography*, *69*, 15–27.

Jähnig, S. C., Brabec, K., Buffagni, A., Erba, S., Lorenz, A. W., Ofenbck, T., et al. (2010). A comparative analysis of restoration measures and their effects on hydromorphology and benthic invertebrates in 26 central and southern European rivers. *Journal of Applied Ecology*, *47*(3), 671–680.

Jähnig, S. C., Brunzel, S., Gacek, S., Lorenz, A. W., & Hering, D. (2009). Effects of re-braiding measures on hydromorphology, floodplain vegetation, ground beetles and benthic invertebrates in mountain rivers. *Journal of Applied Ecology*, *46*(2), 406–416.

Kuhnle, R. A. (1996). Unsteady transport of sand and gravel mixtures. In *Advances in Fluvial Dynamics and Stratigraphy* (pp. 183–201).

Kuhnle, R. A., & Southard, J. B. (1988). Bed load transport fluctuations in a gravel bed laboratory channel. *Water Resources Research*, *24*(2), 247–260.

Le Coz, J., Jodeau, M., Hauet, A., Marchand, B., & Le Boursicaud, R. (2014). Image-based velocity and discharge measurements in field and laboratory river engineering studies using the free FUDAA-LSPIV software. In *Proceedings of the International Conference on Fluvial Hydraulics, RIVER FLOW 2014*.

Leduc, P. (2013). Etude experimentale de la dynamique sedimentaire des rivieres en tresses (Doctoral dissertation), Ecole Doctorale Terre, Univers, Environnement, Universite de Grenoble. NNT: 2013GRENU039. tel-01167872.

Lisle, T. E., Ikeda, H., & Iseya, F. (1991). Formation of stationary alternate bars ina steep channel with mixed-size sediment: A flume experiment. *Earth Surface Processes and Landoforms*, *16*, 463–469.

Lisle, T. E., Nelson, J. M., Pitlick, J., Madej, M. A., & Barkett, B. L. (2000). Variability of bed mobility in natural, gravel-bed channels and adjustments to sediment load at local and reach scales. *Water Resources Reserch*, *36*(12), 3743–3755.

Madej, M. A., Sutherland, D. G., Lisle, T. E., & Pryo, B. (2009). Channel responses to varying sediment input: A flume experiment modeled after Redwood Creek, California. *Geomorphology*, *103*, 507–519.

Marti, C., & Bezzola, G. R. (2006). Bed load transport in braided gravel-bed rivers, *Braided rivers* (pp. 199–215). John Wiley & Sons, Ltd.

Martín, E. J., Ryo, M., Doering, M., & Robinson, C. T. (2018). Evaluation of restoration and flow interactions on river structure and function: Channel widening of the Thur River, Switzerland. *Water*, *10*(4), 439.

Mosselman, E. (2012). *Modelling sediment transport and morphodynamics of gravel-bed rivers*. John Wiley & Sons.

Mueller, E. R., & Pitlick, J. (2014). Sediment supply and channel morphology in mountain river systems: 2. Single thread to braided transitions. *Journal of Geophysical Research: Earth Surface*, *119*, 1516–1541. https://doi.org/10.1002/2013JF003045

Nelson, P. A., McDonald, R. R., Nelson, J. M., & Dietrich, W. E. (2015). Coevolution of bed surface patchiness and channel morphology: 1. Mechanisms of forced patch formation. *Journal of Geophysical Research: Earth Surface*, *120*, 1687–1707. https://doi.org/10.1002/2014JF003428

Nelson, P. A., Venditti, J. G., Dietrich, W. E., Kirchner, J. W., Ikeda, H., Iseya, F., & Sklar, L. S. (2009). Response of bed surface patchiness to reductions in sediment supply. *Journal of Geophysical Research*, *114*, F02005. https://doi.org/10.1029/2008JF001144

Ospina, R., & Marmolejo-Ramos, F. (2019). Performance of some estimators of relative variability. *Frontiers in Applied Mathematics and Statistics*, *5*, 43.

Parker, G. (1978). Self-formed straight rivers with equilibrium banks and mobile bed. Part 2. The gravel river. *Journal of Fluid Mechanics*, *89*(1), 127–146.

Parker, G. (2008). Chapter 18: Mobile and static armor in grevel-bed streams, *Sediment transport morphodinamics, e-book*. University of Minnesota.

Parker, G., Klingeman, P., & McLean, D. (1982). Bedload and size distribution in paved gravel-bed streams. *Journal of the Hydraulics Division (ASCE)*, *108*, 544–571.

Peirce, S., Ashmore, P., & Leduc, P. (2018). The variability in the morphological active width: Results from physical models of gravel-bed braided rivers. *Earth Surface Processes and Landforms*, *43*(11), 2371–2383.

Piton, G., Recking, A., Le Coz, J., Bellot, H., Hauet, A., & Jodeau, M. (2018). Reconstructing depth-averaged open-channel flows using image velocimetry and photogrammetry. *Water Resources Research*, *54*, 4164–4179. https://doi.org/10.1029/2017WR021314

Recking, A. (2012). Influence of sediment supply on mountain streams bedload transport. *Geomorphology*, *175–176*, 139–150.

Recking, A., Frey, P., Paquier, A., & Belleudy, P. (2009). An experimental investigation of mechanisms involved in bed load sheet production and migration. *Journal of Geophysical Research*, *114*, F03010. https://doi.org/10.1029/2008JF000990

Recking, A., Piton, G., Vazquez-Tarrio, D., & Parker, G. (2016). Quantifying the morphological print of bedload transport. *Earth Surface Processes and Landforms*, *41*(6), 809–822.

Rohde, S., Kienast, F., & Bürgi, M. (2004). Assessing the restoration success of river widenings: A landscape approach. *Environmental Management*, *34*(4), 574–589.

Rohde, S., Schtz, M., Kienast, F., & Englmaier, P. (2005). River widening: an approach to restoring riparian habitats and plant species. *River Research and Applications*, *21*(10), 1075–1094.

Singh, A., Fienberg, K., Jerolmack, D. J., Marr, J., & Foufoula-Georgiou, E. (2009). Experimental evidence for statistical scaling and intermittency in sediment transport rates. *Journal of Geophysical Research*, *114*, F01025. https://doi.org/10.1029/2007JF000963

Soille, P. (2013). *Morphological image analysis: Principles and applications*: Springer Science & Business Media.

Venditti, J. G., Nelson, J. M., & Dietrich, W. E. (2008). The domain of bedload sheets. In D. Parsons, J. L. Best & A. Trentesaux (Eds.), *Marine and river dune dynamics* (pp. 315–321). Leeds: Leeds Unversity.

Weber, C., Schager, E., & Peter, A. (2009). Habitat diversity and fish assemblage structure in local river widenings: A case study on a Swiss river. *River Research and Applications*, *25*(6), 687–701.

Whiting, P. J., Dietrich, W. E., Leopold, L. B., Drake, T. G., & Shreve, R. L. (1988). Bedload sheets in heterogeneous sediment. *Geology*, *16*(2), 105–108.

Yager, E. M., Turowski, J. M., Rickenmann, D., & McArdell, B. W. (2012). Sediment supply, grain protrusion, and bedload transport in mountain streams. *Geophysical Research Letters*, *39*, L10402. https://doi.org/10.1029/2012GL051654